Published in final edited form as:
Neuron. 2013 January 9; 77(1): 58–69. doi:10.1016/j.neuron.2012.10.032.

Notch Inhibition Induces Cochlear Hair Cell Regeneration and Recovery of Hearing after Acoustic Trauma

Kunio Mizutari[1,2,‡], **Masato Fujioka**[1,2,3,‡], **Makoto Hosoya**[3], **Naomi Bramhall**[1,2,4], **Hirotaka James Okano**[3], **Hideyuki Okano**[3], and **Albert S.B. Edge**[1,2,4,*]

[1]Department of Otology and Laryngology, Harvard Medical School, Boston MA 02115

[2]Eaton-Peabody Laboratory, Massachusetts Eye and Ear Infirmary, Boston, MA 02114

[3]Department of Physiology, Keio University School of Medicine, Tokyo 160-8582

[4]Program in Speech and Hearing Bioscience and Technology, Division of Health Science and Technology, Harvard & MIT, Cambridge, MA 02139

SUMMARY

Hearing loss due to damage to auditory hair cells is normally irreversible because mammalian hair cells do not regenerate. Here, we show that new hair cells can be induced and can cause partial recovery of hearing in ears damaged by noise trauma, when Notch signaling is inhibited by a γ-secretase inhibitor selected for potency in stimulating hair cell differentiation from inner ear stem cells *in vitro*. Hair cell generation resulted from an increase in the level of bHLH transcription factor, Atoh1, in response to inhibition of Notch signaling. *In vivo* prospective labeling of Sox2-expressing cells with a Cre/lox system unambiguously demonstrated that hair cell generation resulted from transdifferentiation of supporting cells. Manipulating cell fate of cochlear sensory cells *in vivo* by pharmacological inhibition of Notch signaling is thus a potential therapeutic approach to the treatment of deafness.

INTRODUCTION

The cochlear sensory epithelium contains hair cells adapted for the detection of sound, which is transduced by stereocilia at their apical surfaces (Hudspeth, 2008; Nayak et al., 2007). Hair cells produced during development are post-mitotic and are not replaced after loss (Chen and Segil, 1999; Edge and Chen, 2008; Kelley, 2006; Sage et al., 2005) or as part of normal cell turnover in mammals (Corwin and Cotanche, 1988; Fritzsch et al., 2006; Ryals and Rubel, 1988). As a result, deafness due to hair cell loss is irreversible. Hair cell development includes a complex series of fate decisions, in which prosensory epithelial cells acquire different fates, either hair cell or supporting cell, through a process of lateral inhibition which is mediated by Notch signaling (Adam et al., 1998; Daudet and Lewis, 2005; Kelley, 2006). Supporting cells are prevented from differentiating into hair cells by active Notch signaling stimulated by ligands on adjacent hair cells.

*Corresponding author: Albert Edge, Eaton-Peabody Laboratory, Massachusetts Eye and Ear Infirmary, 243 Charles Street, Boston, MA 02114, Tel: (617) 573-4452, Fax: (617) 720-4408, albert_edge@meei.harvard.edu.
‡These authors contributed equally to the study.

Here, we manipulate Notch signaling to generate new hair cells in a deafened animal. Recent insights at the cellular and molecular level have motivated the effort to assess efficacy *in vivo*. One question has been whether there were cells in the damaged cochlea that signaled through the Notch pathway and could serve as precursors for hair cells. Notch signaling has been difficult to detect in the adult cochlea (Batts et al., 2009; Doetzlhofer et al., 2009; Hartman et al., 2009), but some have shown upregulation after damage. In addition, inner ear stem cells isolated postnatally acted as precursors to hair cells when treated with a γ-secretase inhibitor (Jeon et al., 2011). Mechanistic work on the role of Notch revealed a requirement for Atoh1 for the efficacy of the γ-secretase inhibitor, as preventing Atoh1 expression at the time of inhibitor treatment blocked the differentiation to hair cells (Jeon et al., 2011). This was consistent with the result that *Atoh1* overexpression with viruses or plasmids in immature cochleae or adult ototoxic drug-injured cochleae (Gubbels et al., 2008; Izumikawa et al., 2005; Zheng and Gao, 2000) resulted in generation of new hair cells in the organ of Corti.

We approached the problem by identifying a potent γ-secretase inhibitor in an assay with inner ear stem cells and assessing its efficacy first in organ of Corti explants after damage of hair cells and then in a mouse model of deafness. We used a lineage tag to determine the source of the new hair cells. We show that indeed new hair cells were formed after treatment with the inhibitor, that they arose by transdifferentiation of supporting cells, and that the new hair cells contributed to a partial reversal of hearing loss in mice.

RESULTS

Screening for γ-secretase inhibitors that induce hair cell differentiation from inner ear stem cells

Ligand-triggered γ-secretase activity catalyzes proteolytic release of Notch intracellular domain and thereby mediates the first step of Notch signal transduction. We previously showed that γ-secretase inhibitors promoted hair cell differentiation from inner ear stem cells by an effect on Notch (Jeon et al., 2011). To find the most potent inhibitor we tested several known drugs, DAPT, L-685458, MDL28170, and LY411575, for their effect on hair cell differentiation from utricular spheres derived from neonatal *Math1-nGFP* reporter mice (Lumpkin et al., 2003). LY411575 had the highest potency (Figure 1A) among the four γ-secretase inhibitors. To confirm the effect of LY411575 on cochlear cells, we used spheres derived from organ of Corti. Upon treatment with LY411575, the numbers of myosin VIIa-positive cells (myosin VIIa is a specific marker for hair cells) increased 1.5 to 2.5 fold above control (Figure 1B). These cells were also positive for calretinin, another marker for hair cells, and their hair bundles were positive for espin (data not shown).

LY411575 increased hair cell number in organ of Corti explants

We further characterized the effect of LY411575 on neonatal organ of Corti explants. The addition of LY411575 increased the number of myosin VIIa-positive cells in the outer hair cell region (Figure 1C) by 30 cells/100 μm compared to the control (Figure 1D, $p < 0.05$). The additional hair cells showed hair bundle structures. These results indicated that the γ-secretase inhibitor, which was chosen by screening using inner ear stem cells, effectively induced extra hair cell differentiation in the neonatal organ of Corti.

We next used organ of Corti explants from *Pou4f3-Cre*; *Mos-iCsp3* double transgenic mice to test whether hair cells could be induced after damage (Figure 2A). This *Mos-iCsp3* mouse has a Cre/lox cassette that produces a drug-regulated dimerizable caspase-3 (Fujioka et al., 2011) in hair cells, because *Pou4f3*, which is expressed transiently in the developing inner ear, is limited to hair cells (Sage et al., 2006). Thus, after treatment with a drug that

dimerizes caspase-3, the dimer leads to hair cell death. *Mos-iCsp3* cochleae showed loss of outer hair cells (Figure 2B vs Figure 2C, control). LY411575 treatment of *Mos-iCsp3* organ of Corti increased the number of myosin VIIa-positive (hair) cells in the outer hair cell region (Figure 2D; $p < 0.05$) and was accompanied by a decrease in the number of Sox2-positive (supporting) cells in the mid-apex and mid-base of the cochlea (Figure 2D; $p < 0.05$). There were no significant differences in the number of inner hair cells in any group. The correlation between the increase in outer hair cells and the decrease in supporting cells after LY411575 treatment suggested that supporting cells transdifferentiated into hair cells when Notch signaling was prevented.

Systemic LY411575 administration increased hair cell number and promoted hearing recovery in a noise-damaged cochlea

To assess whether hair cell differentiation could be induced in a mature ear, we first exposed mice to an acoustic injury (Wang et al., 2002) producing widespread outer hair cell death and permanent hearing loss with preservation of supporting cells (Figure S1). Oral LY411575 at 50 mg/kg body weight for 5 d decreased the noise-induced threshold shift at 4, 8 and 16 kHz (Figure S2A). Outer hair cell numbers were increased and the new hair cells had stereociliary bundles (Figure S2B). The treated mice suffered significant side-effects (Figure S2B). A lower dose (10 mg/kg body weight) had no therapeutic benefit.

Local LY411575 administration promoted hearing recovery by supporting cell transdifferentiation into hair cells after noise-induced hearing loss in the mature cochlea

Due to the dose-limiting toxicity after systemic administration of the drug, we tested direct delivery to the inner ear via the round window membrane, a permeable cellular barrier between the middle and inner ear (Goycoolea and Lundman, 1997; Salt and Plontke, 2009). We first assessed the time course of *Hes5* and *Atoh1* mRNA expression levels in the deafened mature cochlea in the presence and absence of LY411575 using quantitative RT-PCR. *Hes5* is a direct downstream target of Notch signaling that represses *Atoh1* (Zine et al., 2001). LY411575 was administered *via* the round window niche 1 d after noise exposure. After the noise exposure, *Hes5* mRNA expression increased by 2.15 ± 0.26 compared to its pre-noise level and its level gradually decreased to reach the pre-noise level 3 d after noise exposure (Figure 3A). This induction was completely blocked in the LY411575 treated group at 1 d and stayed at the pre-noise level (significant difference from the control cochlea, $p < 0.01$). Three d after LY411575 treatment, the *Hes5* expression level was unchanged from the control cochlea. In contrast to *Hes5*, *Atoh1* expression remained stable after noise exposure (Figure 3B). Its expression was significantly increased 1 d after LY411575 treatment to 2.28 × above the level post-noise exposure, and remained elevated 3 d after treatment ($p < 0.05$), before returning to the pre-noise level after 7 d. These results showed that a Notch signal could be activated by intense noise trauma, and reduction of *Hes5* in the young adult mouse cochlea by local γ–secretase inhibitor treatment led to sustained upregulation of *Atoh1*.

We used *in vivo* lineage tracing to test whether transdifferentiation could account for new hair cells. We used a Cre-reporter strain to perform lineage tracing of Sox2-positive cells since Sox2 is expressed in supporting cells. In *Sox2-CreER; mT/mG* mice, cells expressing Sox2 at the time of tamoxifen administration become positive for GFP and retain expression even if they lose Sox2 expression (Figure S3). We exposed reporter mice to noise 1 week after tamoxifen treatment, and administered LY411575 to the left ear and carrier to the right ear 1 d after noise exposure. One month after LY411575 treatment, numerous myosin VIIa-positive cells in the deafened cochlea also expressed GFP, demonstrating transdifferentiation from Sox2-positive cells. We observed green hair bundles in the myosin VIIa/GFP double-labeled cells (Figure 4A and B), and some of the bundles appeared in a V-shaped

arrangement like the original hair cells (Figure 4C and C'). Furthermore, the GFP-labeled cells showed positive staining for prestin (Figure 4F), the motor protein of outer hair cells (Dallos et al., 2006), and were negative for VGLUT3, a marker of inner hair cells (Seal et al., 2008), as well as CtBP2 (Figure 4G), a synaptic ribbon marker that would be expected to be expressed if the new hair cells were active inner hair cells (Khimich et al., 2005; Liberman et al., 2011). This analysis of markers together with their location and V-shaped bundles identified them as outer hair cells. These double-labeled cells spanned the epithelium from basilar membrane to the endolymphatic surface (Figure 4D), which is never seen in the normal ear, but has been reported when supporting cells are transfected with Atoh1 (Izumikawa et al., 2005). The nucleus of these cells was at the base of the cell (Figure 4D'). Double-labeled cells were found in the upper turns of the cochlea, with the highest numbers in the mid apex (Figure 4E; n = 5). In control ears, no double-labeled cells were observed in any cochlear region (Figure S3). This result indicated that blocking Notch with LY411575 promoted supporting cell transdifferentiation into hair cells from the apical to mid-apical turn in the mature cochlea after noise-induced hair cell loss.

At 3 months the number of outer hair cells was increased throughout the middle of the cochlea (8 – 16 kHz) in LY411575 treated ears, compared to the carrier-treated contralateral ear (Figure 5A and B; $p < 0.05$). The number of supporting cells in the outer hair cell region was decreased significantly in the same cochleae as the increase in outer hair cell number at the 8 and 11.3 kHz areas compared to the carrier-treated ear (Figure 5A and B; $p < 0.05$). Decreases in supporting cells were also significant (Figure 5B, $p < 0.05$) similar to the explant cultures. The outer hair cells were completely absent with and without LY411575 treatment in the most basal regions (above 22 kHz), and there were no significant changes in the numbers of inner hair cells in the treated group (data not shown). The differences in outer hair cell number between LY411575 and carrier-treated ears are larger than the corresponding differences in the number of supporting cells. Furthermore, the differences in outer hair cell number showed a similar trend, in regard to cochlear location, as the myosin VIIa-positive cells from the Sox2-lineage observed in *Sox2-CreER*; *mT/mG* mice (Figure 4E).

We recorded the auditory brainstem response (ABR) in LY411575 and carrier-treated, control ears to determine the effect of hair cell replacement on the thresholds for a response. Threshold changes were not seen after injection of carrier alone (Figure S4). ABR thresholds 1 d after noise-exposure were >80 dB SPL at all frequencies (Figure 6A and B). Post-exposure recovery in control ears (Fig. 6A) was minimal under these conditions, as expected (Wang et al., 2002). Threshold recoveries after LY411575 treatment were significantly greater than control at 8, 11.33 and 16 kHz (Figure 6D), and wave I amplitudes were increased at the same frequencies (Figure 6E). No threshold recoveries were observed in either ear at frequencies above 22.65 kHz by ABR and no recoveries above the noise floor of the distortion product otoacoustic emissions (DPOAE) could be seen (Figure S5). The differences in threshold recovery showed a similar dependence on cochlear location/ frequency as outer hair cell number (see Figure 5).

DISCUSSION

We have demonstrated significant regeneration of hair cells in a mammal by treatment of a damaged cochlea with a γ-secretase inhibitor. *In vivo* treatment with the inhibitor resulted in partial recovery after noise-induced hearing loss.

The generation of physiologically active hair cells in an adult has been a sought-after but elusive goal. Transfection of bHLH transcription factor, Atoh1, which drives hair cell differentiation during development, is one approach that increases hair cell number in

embryonic or newborn tissue, but cells that were competent to become hair cells in the embryo lost their responsiveness as the animal matured (Doetzlhofer et al., 2009; Gubbels et al., 2008; White et al., 2006). Delivery of Atoh1 in an adenovirus to the damaged, adult cochlea (Izumikawa et al., 2005) showed some hair cell differentiation, but the number of new hair cells was not clear and new hair cells could not be traced from their precursors, making it difficult to distinguish between "new" hair cells and hair cells that had recovered from trauma due to a toxin or noise damage. Stimulation of cell division by silencing cell cycle inhibitors has been suggested as an alternative route to hair cell regeneration (Sage et al., 2005), but hair cells, due to their highly differentiated state, tend to activate suicide programs after they divide and proliferation can cause deafness (Chen and Segil, 1999; Lowenheim et al., 1999; Mantela et al., 2005). Regeneration of hair cells is made difficult by the cellular organization of the cochlea: minute changes in the interactions between cells of the epithelium are a cause of deafness (Cohen-Salmon et al., 2002). Tight junctions are required for maintaining the ionic milieu of endolymph that bathes the surface of hair cells, and the flexibility and spacing of outer hair cells has an impact on the function of the cochlear amplifier, which is achieved by outer hair cell contraction, and together with sound detection by the transduction apparatus of inner hair cells, accounts for the sensitivity and broad dynamic range of mammalian hearing (Elgoyhen and Franchini, 2011; Hudspeth, 2008; Richardson et al., 2011).

We had recently shown that inhibition of Notch increased hair cell differentiation from stem cells and that the mechanism was dependent on Atoh1, since silencing the transcription factor in the γ-secretase inhibitor-treated stem cells prevented the induction of hair cell fate (Jeon et al., 2011). We used inner ear stem cells to select a potent γ-secretase inhibitor. We targeted the Notch pathway, which would only be effective on cells that were actively signaling through Notch. Although increased Notch signaling in the adult after damage had been suggested by some (Batts et al., 2009), the loss of an effect of γ-secretase inhibitors on hair cell number in the early postnatal period (Doetzlhofer et al., 2009) and data suggesting that Notch signaling was extinguished after birth (Hartman et al., 2009) both suggested that γ-secretase inhibitors would have no effect on hair cell number in the adult mammalian cochlea.

However, we have shown that inhibition of Notch after noise damage leads to transdifferentiation of supporting cells into hair cells. The basal location of the nucleus in the new hair cells was consistent with the derivation from supporting cells, which are normally located in a plane below that of the hair cells. Supporting cell transdifferentiation was induced by Atoh1, which may be acting in a similar capacity to transcription factors, some of which are related to Atoh1, that allow cellular reprogramming and transdifferentiation to neurons (Caiazzo et al., 2011; Vierbuchen et al., 2010). The supporting cells express stem cell markers such as Sox2, Musashi1, and GLAST (Kaneko et al., 2000; Oesterle et al., 2008; Sakaguchi et al., 2004) and have the capacity for proliferation and transdifferentiation for a short period postnatally (White et al., 2006). Capacity for neurosphere formation by the sensory epithelial cells in the cochlea is found in a similar postnatal time frame (Oshima et al., 2007).

Both the cellular and molecular aspects of hair cell regeneration in the adult mammalian cochlea were similar to observations in lower vertebrates (Stone and Cotanche, 2007; Warchol, 2010), where supporting cells act as precursors for hair cells under the influence of Atoh1 (Cafaro et al., 2007). In birds, some cells respond by entering the cell cycle and transdifferentiating, whereas others do not respond on their own but undergo transdifferentiation if treated with a γ-secretase inhibitor (Daudet et al., 2009). In the mouse the mechanism leading to hair cell differentiation in the cochlea was upregulation of Atoh1 due to inhibition of the Notch activity stimulated by the acute damage, and supporting cells

acted as progenitors for hair cells. Indeed, transdifferentiation has also been described in utricle explants from newborn mice after γ-secretase inhibitor treatment (Lin et al., 2011).

Drug therapy for restoration of hair cells is a new approach and the delivery to the inner ear fluids without actual injection into the cochlea may be an advantage over gene therapy and may also effectively restrict hair cell differentiation to cells in the sensory epithelial area as compared to gene therapy that may convert hair cells in a broader area. We decided to use a middle ear approach for the delivery of LY411575 to the damaged inner ear because of the severe side effects when it was administrated systemically. Since the round window membrane consists of cell layers, lipid solubility of the drug favors permeability (Goycoolea and Lundman, 1997; Salt and Plontke, 2009). A potential issue is the loss of supporting cells that become hair cells, and it may be necessary to replace supporting cells for an optimal, long-term effect. We found that the recovery lasted for at least 3 months, our longest time point. The approach may be limited to treatment of acute hearing loss after damage and may be less effective after longer time periods when Notch signaling has returned to its baseline level in the adult.

Novel approaches using inner ear stem cells and transgenic mice were critical for our demonstration that hair cells could regenerate in the mouse. The caspase-3 mouse provided a model in which we could kill hair cells without damage to other cells so that we could quantify new hair cells. Lineage tracing with the *mT/mG*; *Sox2-CreER* double transgenic mouse allowed us to show unambiguously that drug treatment resulted in new hair cells and not recovery of hair cell bundles that could have accounted for recovery in the absence of lineage tracing. Improved thresholds were found by ABR, showing that hearing was improved by γ-secretase inhibitor administration in the acute damage situation. Hair cell counts showed an increase in the same frequency regions as the improved ABR. Thus we used the frequency specificity of the improved hearing to determine the correlation between the gain in hair cell number and the improved hearing threshold. The damage in the acute noise-exposure model reflected hair cell loss in humans, most severe in the base and restricted primarily to the outer hair cells (Wang et al., 2002). The improvement in threshold at the apex of the cochlea was thought to result from an increase in the number of hair cells to a level that produced a detectable change through outer hair cell activity. As a result of the greater damage at the base of the cochlea, the number of hair cells at the base was not adequate to lower the threshold of the ABR, and the increase in hair cells in the apex could not be detected by a change in DPOAE threshold. The combined physiological and cellular evidence allowed a definitive proof of the regeneration of hair cells that was quantitative, was correlated to frequency, and provided unequivocal evidence as to the genesis of the hair cells by lineage tracing from supporting cells.

EXPERIMENTAL PROCEDURES

Animals

For the experiments using inner ear spheres, C57BL/6 (Jackson Labs) or *Math1-nGFP* reporter mouse (Lumpkin et al., 2003) (a gift from Jane Johnson, University of Texas) of both sexes were used. To create organ of Corti explants with ablated hair cells, *Mos-iCsp3* mice (line 17) (Fujioka et al., 2011) were crossed with *Pou4f3-Cre* mice (Sage et al., 2005) (a gift from Douglas Vetter, Tufts University). For all *in vivo* experiments, we used 4-week-old *Cre* reporter line, *mT/mG* (Jackson Labs), crossed to a *Sox2-CreER* mouse (Arnold et al., 2011) (a gift from Konrad Hochedlinger, Mass General Hospital). After genotyping, double transgenic animals were used for lineage tracing. We used young adult wild-type littermates of the *mT/mG*; *Sox2-CreER* mice to prevent strain effects in the response to noise, which are known to vary depending on background (Harding et al., 2005; Wang et al., 2002). Mice were genotyped by PCR. All protocols were approved by the Institutional

Animal Care and Use Committee of Massachusetts Eye and Ear Infirmary or the by the ethics committee of Keio University Union on Laboratory Animal Medicine, in compliance with the Public Health Service policy on humane care and use of laboratory animals.

Isolation of inner ear spheres

The utricles and cochleae of 1- to 3-d-postnatal mice of both sexes were dissected, and after careful removal of the nerve trunk and mesenchymal tissues, were trypsinized and dissociated. Dissociated cells were centrifuged, and the pellet was resuspended and filtered through a 70 μm cell strainer (BD Biosciences Discovery Labware) in DMEM/F12 medium with N2/B27 supplement, EGF (20 ng/ml), IGF1 (50 ng/ml), bFGF (10 ng/ml), and heparan sulfate (50 ng/ml) (Sigma). The single cells were cultured in nonadherent Petri dishes (Greiner Bio-One) to initiate clonal growth of spheres (Martinez-Monedero et al., 2008). Spheres that formed after 2–3 d in culture were passaged every 4–6 d. The spheres were centrifuged, and the pellet was mechanically dissociated with a pipette tip and resuspended in medium. Passage 3–4 spheres were used for experiments described here. These cells are negative for hair cell markers (Oshima et al., 2007) before the initiation of differentiation. For differentiation, floating spheres were transferred to fibronectin-coated 4 well plates (Greiner Bio-One) as described before (Martinez-Monedero et al., 2008; Oshima et al., 2007). Attached spheres were differentiated for 5–7 d in DMEM/F12 medium with N2/B27 supplement but without growth factors.

Gamma-secretase inhibitors, DAPT, L-685458, MDL28170 (Sigma), and LY411575 (Santa Cruz) were added at several concentrations on the day following cell attachment.

Neonatal cochlear explants

Cochleae of 3-d-postnatal C57BL/6 or *Mos-iCsp3*; *Pou4f3-Cre* double transgenic mice of both sexes were dissected in Hanks solution (Invitrogen). To obtain a flat cochlear surface preparation, the spiral ganglion, Reissner's membrane, and the most basal cochlear segment were removed. Explants were plated onto 4 well plates (Greiner Bio-One) coated with poly-L-ornithine (0.01%, Sigma) and laminin (50 μg/ml, Becton Dickinson). Cochlear explants were cultured in DMEM (Invitrogen) with 10% fetal bovine serum. All cultures were maintained in a 5% CO2/20% O2-humidified incubator (Forma Scientific).

Acoustic overexposure

4-week-old mice were exposed free-field, awake and unrestrained, in a small reverberant chamber (Wang et al., 2002). Acoustic trauma was produced by a 2 h exposure to an 8–16 kHz octave band noise presented at 116 dB SPL. The exposure stimulus was generated by a custom white-noise source, filtered (Brickwall Filter with a 60 dB/octave slope), amplified (Crown power amplifier), and delivered (JBL compression driver) through an exponential horn fitted securely to a hole in the top of a reverberant box. Sound exposure levels were measured at four positions within each cage using a 0.25 inch Brüel and Kjær condenser microphone: sound pressure was found to vary by <0.5 dB across these measurement positions.

Systemic or round window administration of LY411575

4-week-old mice weighing 12 to 16 g were used. Before surgery, the animals were anesthetized with ketamine (20 mg/kg, i.p.) and xylazine (100 mg/kg, i.p.), and an incision was made posterior to the pinna near the external meatus after local administration of lidocaine (1%). The otic bulla was opened to approach the round window niche. The end of a piece of PE 10 tubing (Becton Dickinson) was drawn to a fine tip in a flame and gently inserted into the round window niche. LY411575 was dissolved in DMSO and diluted 10-

fold in polyethylene glycol 400 (Sigma) to a final concentration of 4 mM. This solution (total volume 1 μl) was injected into the round window niche of the left ear. Polyethylene glycol 400 with 10% DMSO was injected into the right ear as a control. The solution was administered for 2 min. This approach is widely used clinically and has the advantage of sparing the inner ear but still taking advantage of the local route provided by the round window membrane for delivery of drug into the inner ear (Mikulec et al., 2008). Gelatin was placed on the niche to maintain the solution, and the wound was closed.

For the systemic administration, LY411575 (50 mg/kg) dissolved in 0.5% (wt/vol) methylcellulose (WAKO) was injected orally once daily for 5 consecutive d. Hearing was measured by ABR at 1 d before, 2 d, 1, 2 week, 1, 2 and 3 months after noise exposure.

qRT-PCR

The organs of Corti were dissected in HBSS (Invitrogen) and stored in RNAlater (Ambion) at −80° C until further use. Total RNA was extracted using the RNeasy Mini Kit (Qiagen) according to the manufacturer's instructions. For reverse transcription, SuperScript II (Invitrogen) was used with random hexamers. The reverse transcription conditions were 25° C for 10 min followed by 37° C for 60 min. The reaction was terminated at 95°C for 5 min. cDNAs were mixed with Taqman Gene Expression Mastermix (Applied Biosystems) and *Hes5, Atoh1*, or *18S* primers (Applied Biosystems) according to the manufacturer's instructions. Samples were analyzed in 96 wells in triplicate by qPCR (Applied Biosystems 7900HT), and PCR thermal cycling conditions were as follows: initial denaturation at 95° C for 2 min, denaturation at 95°C for 15 s, annealing/extension at 60° C for 1 min for 45 cycles. Conditions were kept constant for each primer. Each PCR reaction was carried out in triplicate. Relative gene expression was analyzed by using the $\Delta\Delta C_T$ method. Gene expression was calculated relative to 18S RNA, and the amount of cDNA applied was adjusted so that the *C*t value for 18S RNA was between 8 and 11.

Immunohistochemistry

For spheres, cells were fixed for 10 min with 4% paraformaldehyde in PBS. Immunostaining was initiated by blocking for 1 h with 0.1% Triton X-100 in PBS supplemented with 1% BSA and 5% goat serum (PBT1). Fixed and permeabilized cells were incubated overnight in PBT1 with polyclonal antibody to myosin VIIa (Proteus Biosciences). Samples were washed three times for 20 min with PBS. Primary antibodies were detected with secondary antibodies conjugated with Alexa 488 (Molecular Probes), with secondary antibody alone used as a negative control. The samples were counterstained with DAPI (Vector Laboratories) or Hoechst 33258 (Invitrogen) for 10 min and viewed by epifluorescence microscopy (Axioskop 2 Mot Axiocam, Zeiss).

For explants, the organs of Corti were fixed for 15 min with 4% paraformaldehyde in PBS. Immunostaining was initiated by blocking the tissues for 1 h with 0.1% Triton X-100 in PBS supplemented with 5% donkey serum (PBT1). Fixed and permeabilized pieces were incubated overnight in PBT1 with polyclonal antibody to myosin VIIa (Proteus Biosciences), Sox2 (Santa Cruz), GFP (Invitrogen), prestin (Santa Cruz), and CtBP2 (BD Biosciences). Samples were washed three times for 20 min with PBS. Primary antibodies were detected with secondary antibodies conjugated with Alexa 488 and 647 (Molecular Probes). The samples were stained with rhodamine phalloidin (Invitrogen) for 15 min and viewed by confocal fluorescence microscopy (TCS SP5, Leica).

For collection of mature mouse cochleae, after being deeply anesthetized with ketamine and xylazine, the mice were transcardially perfused with 0.01 M phosphate buffer (pH 7.4) containing 8.6% sucrose, followed by fixative consisting of freshly depolymerized 4%

paraformaldehyde in 0.1 M phosphate buffer (pH 7.4). After decapitation, the temporal bones were removed and immediately placed in the same fixative at 4° C. Small openings were made at the round window, oval window, and apex of the cochlea. After immersion in the fixative overnight at 4° C, temporal bones were decalcified in 0.1 M EDTA (pH 7.4) containing 5% sucrose with stirring at 4° C for 2 d. After decalcification, cochleae were microdissected into 4 pieces for whole mount preparation. Immunostaining was initiated by blocking the tissues for 1 h with 0.1% Triton X-100 in PBS supplemented with 5% donkey serum (PBT1). Fixed and permeabilized pieces were incubated overnight in PBT1 with polyclonal antibody to myosin VIIa (Proteus Biosciences), Sox2 (Santa Cruz), and GFP (Invitrogen). Samples were washed three times for 20 min with PBS. Primary antibodies were detected with secondary antibodies conjugated with Alexa 488, 568, and 647 (Molecular Probes) and viewed by confocal fluorescence microscopy (TCS SP5, Leica). Cochlear lengths were obtained for each case, and a cochlear frequency map computed to precisely localize inner hair cells from the 5.6, 8.0, 11.3, 16.0, 22.6, 32, and 45.2 kHz regions. For cross-sectioning, fixed temporal bones were sunk in 30% sucrose in PBS at 4°C, incubated in OCT at room temperature for 1 h, and frozen in liquid nitrogen. The staining protocol was the same as described above except for counterstaining with DAPI (Vector Laboratories). Specimens were viewed by epifluorescence microscopy (Axioskop 2 Mot Axiocam, Zeiss).

Cell Counts

Cell counting for spheres was performed with MetaMorph software. The cell number was determined from DAPI- or Hoechst-positive nuclei. Repeat cell counting gave a test variation of <1%. For explants, inner hair cells, outer hair cells, and supporting cells in the outer hair cell region were counted on cochlear whole mounts. Hair cells were identified with myosin VIIa antibodies or endogenous GFP in *Math1-nGFP* mice. High-power images of the full-length cochlea or cochlear explant cultures were assembled and analyzed in PhotoShop CS4 (Adobe). ImageJ software (NIH) was used to measure the total length of cochlear whole mounts and the length of individual counted segments. The total number of inner hair cells, outer hair cells, and supporting cells in the outer hair cell region was counted in each of four cochlear segments of 1200–1400 μm (apical, mid-apical, mid-basal, and basal). Density (cells per 100 μm) was then calculated for each segment. For mature cochleae, high-power images of frequency-specific regions (5.6, 8.0, 11.3, 16.0 kHz) according to the computed frequency map were assembled and analyzed. The number of inner hair cells, outer hair cells, and supporting cells in the outer hair cell region in 100 μm was counted in each of the four frequency-specific regions of the cochlea. The number of Sox2-lineage-positive cells identified by GFP was counted by the same method.

ABR measurements

Auditory brain stem responses (Kujawa and Liberman, 1997; Maison et al., 2003) were measured in each animal at 7 log-spaced frequencies (half-octave steps from 5.6 to 45.2 kHz) before and 1 d after noise exposure, and 1-week, 1-month, and 3-months after surgery. Mice were anesthetized with ketamine (100 mg/kg i.p.) and xylazine (20 mg/kg i.p.). Needle electrodes were inserted at vertex and pinna, with a ground near the tail. ABRs were evoked with 5-ms tone pips (0.5-ms rise-fall with a $\cos^2$ onset envelope delivered at 35/s). The response was amplified, filtered and averaged in a LabVIEW-driven data-acquisition system. Sound level was raised in 5 dB steps from ≥10 dB below threshold <80 dB SPL. At each sound level, 1024 responses were averaged (with stimulus polarity alternated), using an “artifact reject,” whereby response waveforms were discarded when peak-to-peak response amplitude exceeded 15 μV. On visual inspection of stacked waveforms, “ABR threshold” was defined as the lowest SPL level at which any wave could be detected, usually corresponding to the level step just below that at which the peak-to-peak response

amplituderose significantly above the noise floor (approximately 0.25 μV). When no response was observed at the highest sound level available, the threshold was designated as being 5 dB greater than that level so that statistical tests could be done. For amplitude versus level functions, the wave I peak was identified by visual inspection at each sound level and the peak-to-peak amplitude computed.

Quantification and statistical analysis

The 2-tailed Mann-Whitney U test was used to compare differences among treatment groups. Changes before and after treatment of the same animal were analyzed by 2-tailed Wilcoxon *t* test. Repeated-measures ANOVA was used to compare time-dependent differences among groups. Data are presented in the text and in figures as mean ± SEM. P values less than 0.05 were considered significant.

Genotyping primersv

Mos-iCsp3

LacZ F: 5'-ttcactggccgtcgttttacaacgtcgtga-3'

LacZ R: 5'-atgtgagcgagtaacaacccgtcggattct-3'

Pou4f3Cre, Sox2CreER

Cre F: 5'-tgggcggcatggtgcaagtt-3'

Cre R: 5'-cggtgctaaccagcgttttc-3'

mT/mG

oIMR7318 wild-type F: 5'-ctctgctgcctcctggcttct-3'

oIMR7319 wild-type R: 5'-cgaggcggatcacaagcaata-3'

oIMR7320 mutant R: 5'-tcaatgggcgggggtcgtt-3'

Supplementary Material

Refer to Web version on PubMed Central for supplementary material.

Acknowledgments

We thank M.C. Liberman for critical comments on the manuscript. We thank Yukiko Watada for assistance. This work was supported by grants RO1 DC007174, R21 DC010440-01 and P30 DC05209 from the National Institute on Deafness and other Communicative Disorders (NIDCD), the Mochida Memorial Foundation for Medical and Pharmaceutical Research, and Grants for International Activities in Life Sciences and Medicine, Keio University Medical Science Fund.

REFERENCES

Adam J, Myat A, Le Roux I, Eddison M, Henrique D, Ish-Horowicz D, Lewis J. Cell fate choices and the expression of Notch, Delta and Serrate homologues in the chick inner ear: parallels with Drosophila sense-organ development. Development. 1998; 125:4645–4654. [PubMed: 9806914]

Arnold K, Sarkar A, Yram MA, Polo JM, Bronson R, Sengupta S, Seandel M, Geijsen N, Hochedlinger K. Sox2(+) adult stem and progenitor cells are important for tissue regeneration and survival of mice. Cell Stem Cell. 2011; 9:317–329. [PubMed: 21982232]

Batts SA, Shoemaker CR, Raphael Y. Notch signaling and Hes labeling in the normal and drug-damaged organ of Corti. Hear Res. 2009; 249:15–22. [PubMed: 19185606]

Cafaro J, Lee GS, Stone JS. Atoh1 expression defines activated progenitors and differentiating hair cells during avian hair cell regeneration. Dev Dyn. 2007; 236:156–170. [PubMed: 17096404]

Caiazzo M, Dell'Anno MT, Dvoretskova E, Lazarevic D, Taverna S, Leo D, Sotnikova TD, Menegon A, Roncaglia P, Colciago G, et al. Direct generation of functional dopaminergic neurons from mouse and human fibroblasts. Nature. 2011; 476:224–227. [PubMed: 21725324]

Chen P, Segil N. p27(Kip1) links cell proliferation to morphogenesis in the developing organ of Corti. Development. 1999; 126:1581–1590. [PubMed: 10079221]

Cohen-Salmon M, Ott T, Michel V, Hardelin JP, Perfettini I, Eybalin M, Wu T, Marcus DC, Wangemann P, Willecke K, et al. Targeted ablation of connexin26 in the inner ear epithelial gap junction network causes hearing impairment and cell death. Curr Biol. 2002; 12:1106–1111. [PubMed: 12121617]

Corwin JT, Cotanche DA. Regeneration of sensory hair cells after acoustic trauma. Science. 1988; 240:1772–1774. [PubMed: 3381100]

Dallos P, Zheng J, Cheatham MA. Prestin and the cochlear amplifier. J Physiol. 2006; 576:37–42. [PubMed: 16873410]

Daudet N, Gibson R, Shang J, Bernard A, Lewis J, Stone J. Notch regulation of progenitor cell behavior in quiescent and regenerating auditory epithelium of mature birds. Dev Biol. 2009; 326:86–100. [PubMed: 19013445]

Daudet N, Lewis J. Two contrasting roles for Notch activity in chick inner ear development: specification of prosensory patches and lateral inhibition of hair-cell differentiation. Development. 2005; 132:541–551. [PubMed: 15634704]

Doetzlhofer A, Basch ML, Ohyama T, Gessler M, Groves AK, Segil N. Hey2 regulation by FGF provides a Notch-independent mechanism for maintaining pillar cell fate in the organ of Corti. Dev Cell. 2009; 16:58–69. [PubMed: 19154718]

Edge AS, Chen ZY. Hair cell regeneration. Curr Opin Neurobiol. 2008; 18:377–382. [PubMed: 18929656]

Elgoyhen AB, Franchini LF. Prestin and the cholinergic receptor of hair cells: positively-selected proteins in mammals. Hear Res. 2011; 273:100–108. [PubMed: 20056140]

Fritzsch B, Beisel KW, Hansen LA. The molecular basis of neurosensory cell formation in ear development: a blueprint for hair cell and sensory neuron regeneration? Bioessays. 2006; 28:1181–1193. [PubMed: 17120192]

Fujioka M, Tokano H, Fujioka KS, Okano H, Edge AS. Generating mouse models of degenerative diseases using Cre/lox-mediated in vivo mosaic cell ablation. J Clin Invest. 2011; 121:2462–2469. [PubMed: 21576819]

Goycoolea MV, Lundman L. Round window membrane. Structure function and permeability: a review. Microsc Res Tech. 1997; 36:201–211. [PubMed: 9080410]

Gubbels SP, Woessner DW, Mitchell JC, Ricci AJ, Brigande JV. Functional auditory hair cells produced in the mammalian cochlea by in utero gene transfer. Nature. 2008; 455:537–541. [PubMed: 18754012]

Harding GW, Bohne BA, Vos JD. The effect of an age-related hearing loss gene (Ahl) on noise-induced hearing loss and cochlear damage from low-frequency noise. Hear Res. 2005; 204:90–100. [PubMed: 15925194]

Hartman BH, Basak O, Nelson BR, Taylor V, Bermingham-McDonogh O, Reh TA. Hes5 expression in the postnatal and adult mouse inner ear and the drug-damaged cochlea. J Assoc Res Otolaryngol. 2009; 10:321–340. [PubMed: 19373512]

Hudspeth AJ. Making an effort to listen: mechanical amplification in the ear. Neuron. 2008; 59:530–545. [PubMed: 18760690]

Izumikawa M, Minoda R, Kawamoto K, Abrashkin KA, Swiderski DL, Dolan DF, Brough DE, Raphael Y. Auditory hair cell replacement and hearing improvement by Atoh1 gene therapy in deaf mammals. Nat Med. 2005; 11:271–276. [PubMed: 15711559]

Jeon SJ, Fujioka M, Kim SC, Edge ASB. Notch signaling alters sensory or neuronal cell fate specification of inner ear stem cells. J Neurosci. 2011; 31:8351–8358. [PubMed: 21653840]

Kaneko Y, Sakakibara S, Imai T, Suzuki A, Nakamura Y, Sawamoto K, Ogawa Y, Toyama Y, Miyata T, Okano H. Musashi1: an evolutionally conserved marker for CNS progenitor cells including neural stem cells. Dev Neurosci. 2000; 22:139–153. [PubMed: 10657706]

Kelley MW. Regulation of cell fate in the sensory epithelia of the inner ear. Nat Rev Neurosci. 2006; 7:837–849. [PubMed: 17053809]

Khimich D, Nouvian R, Pujol R, Tom Dieck S, Egner A, Gundelfinger ED, Moser T. Hair cell synaptic ribbons are essential for synchronous auditory signalling. Nature. 2005; 434:889–894. [PubMed: 15829963]

Kujawa SG, Liberman MC. Conditioning-related protection from acoustic injury: effects of chronic deefferentation and sham surgery. J Neurophysiol. 1997; 78:3095–3106. [PubMed: 9405529]

Liberman LD, Wang H, Liberman MC. Opposing gradients of ribbon size and AMPA receptor expression underlie sensitivity differences among cochlear-nerve/hair-cell synapses. J Neurosci. 2011; 31:801–808. [PubMed: 21248103]

Lin V, Golub JS, Nguyen TB, Hume CR, Oesterle EC, Stone JS. Inhibition of Notch activity promotes nonmitotic regeneration of hair cells in the adult mouse utricles. J Neurosci. 2011; 31:15329–15339. [PubMed: 22031879]

Lowenheim H, Furness DN, Kil J, Zinn C, Gultig K, Fero ML, Frost D, Gummer AW, Roberts JM, Rubel EW, et al. Gene disruption of p27(Kip1) allows cell proliferation in the postnatal and adult organ of corti. Proc Natl Acad Sci U S A. 1999; 96:4084–4088. [PubMed: 10097167]

Lumpkin EA, Collisson T, Parab P, Omer-Abdalla A, Haeberle H, Chen P, Doetzlhofer A, White P, Groves A, Segil N, et al. Math1-driven GFP expression in the developing nervous system of transgenic mice. Gene Expr Patterns. 2003; 3:389–395. [PubMed: 12915300]

Maison SF, Emeson RB, Adams JC, Luebke AE, Liberman MC. Loss of alpha CGRP reduces sound-evoked activity in the cochlear nerve. J Neurophysiol. 2003; 90:2941–2949. [PubMed: 12904337]

Mantela J, Jiang Z, Ylikoski J, Fritzsch B, Zacksenhaus E, Pirvola U. The retinoblastoma gene pathway regulates the postmitotic state of hair cells of the mouse inner ear. Development. 2005; 132:2377–2388. [PubMed: 15843406]

Martinez-Monedero R, Yi E, Oshima K, Glowatzki E, Edge AS. Differentiation of inner ear stem cells to functional sensory neurons. Dev Neurobiol. 2008; 68:669–684. [PubMed: 18278797]

Mikulec AA, Hartsock JJ, Salt AN. Permeability of the round window membrane is influenced by the composition of applied drug solutions and by common surgical procedures. Otol Neurotol. 2008; 29:1020–1026. [PubMed: 18758387]

Nayak GD, Ratnayaka HS, Goodyear RJ, Richardson GP. Development of the hair bundle and mechanotransduction. Int J Dev Biol. 2007; 51:597–608. [PubMed: 17891720]

Oesterle EC, Campbell S, Taylor RR, Forge A, Hume CR. Sox2 and JAGGED1 expression in normal and drug-damaged adult mouse inner ear. J Assoc Res Otolaryngol. 2008; 9:65–89. [PubMed: 18157569]

Oshima K, Grimm CM, Corrales CE, Senn P, Martinez Monedero R, Geleoc GS, Edge A, Holt JR, Heller S. Differential distribution of stem cells in the auditory and vestibular organs of the inner ear. J Assoc Res Otolaryngol. 2007; 8:18–31. [PubMed: 17171473]

Richardson GP, de Monvel JB, Petit C. How the genetics of deafness illuminates auditory physiology. Annu Rev Physiol. 2011; 73:311–334. [PubMed: 21073336]

Ryals BM, Rubel EW. Hair cell regeneration after acoustic trauma in adult Coturnix quail. Science. 1988; 240:1774–1776. [PubMed: 3381101]

Sage C, Huang M, Karimi K, Gutierrez G, Vollrath MA, Zhang DS, Garcia-Anoveros J, Hinds PW, Corwin JT, Corey DP, et al. Proliferation of functional hair cells in vivo in the absence of the retinoblastoma protein. Science. 2005; 307:1114–1118. [PubMed: 15653467]

Sage C, Huang M, Vollrath MA, Brown MC, Hinds PW, Corey DP, Vetter DE, Chen ZY. Essential role of retinoblastoma protein in mammalian hair cell development and hearing. Proc Natl Acad Sci U S A. 2006; 103:7345–7350. [PubMed: 16648263]

Sakaguchi H, Yaoi T, Suzuki T, Okano H, Hisa Y, Fushiki S. Spatiotemporal patterns of Musashi1 expression during inner ear development. Neuroreport. 2004; 15:997–1001. [PubMed: 15076722]

Salt AN, Plontke SK. Principles of local drug delivery to the inner ear. Audiol Neurootol. 2009; 14:350–360. [PubMed: 19923805]

Seal RP, Akil O, Yi E, Weber CM, Grant L, Yoo J, Clause A, Kandler K, Noebels JL, Glowatzki E, et al. Sensorineural deafness and seizures in mice lacking vesicular glutamate transporter 3. Neuron. 2008; 57:263–275. [PubMed: 18215623]

Stone JS, Cotanche DA. Hair cell regeneration in the avian auditory epithelium. Int J Dev Biol. 2007; 51:633–647. [PubMed: 17891722]

Vierbuchen T, Ostermeier A, Pang ZP, Kokubu Y, Sudhof TC, Wernig M. Direct conversion of fibroblasts to functional neurons by defined factors. Nature. 2010; 463:1035–1041. [PubMed: 20107439]

Wang Y, Hirose K, Liberman MC. Dynamics of noise-induced cellular injury and repair in the mouse cochlea. J Assoc Res Otolaryngol. 2002; 3:248–268. [PubMed: 12382101]

Warchol ME. Sensory regeneration in the vertebrate inner ear: Differences at the levels of cells and species. Hear Res. 2010

White PM, Doetzlhofer A, Lee YS, Groves AK, Segil N. Mammalian cochlear supporting cells can divide and trans-differentiate into hair cells. Nature. 2006; 441:984–987. [PubMed: 16791196]

Zheng JL, Gao WQ. Overexpression of Math1 induces robust production of extra hair cells in postnatal rat inner ears. Nat Neurosci. 2000; 3:580–586. [PubMed: 10816314]

Zine A, Aubert A, Qiu J, Therianos S, Guillemot F, Kageyama R, de Ribaupierre F. Hes1 and Hes5 activities are required for the normal development of the hair cells in the mammalian inner ear. J Neurosci. 2001; 21:4712–4720. [PubMed: 11425898]

HIGHLIGHTS

- Sensory hair cell regeneration is demonstrated for the first time in an adult mammal.
- Inhibition of Notch stimulates hair cell regeneration after acoustic trauma.
- Hair cells are derived from transdifferentiation of cochlear supporting cells.
- Frequency region of hearing recovery corresponds to area of hair cell replacement.

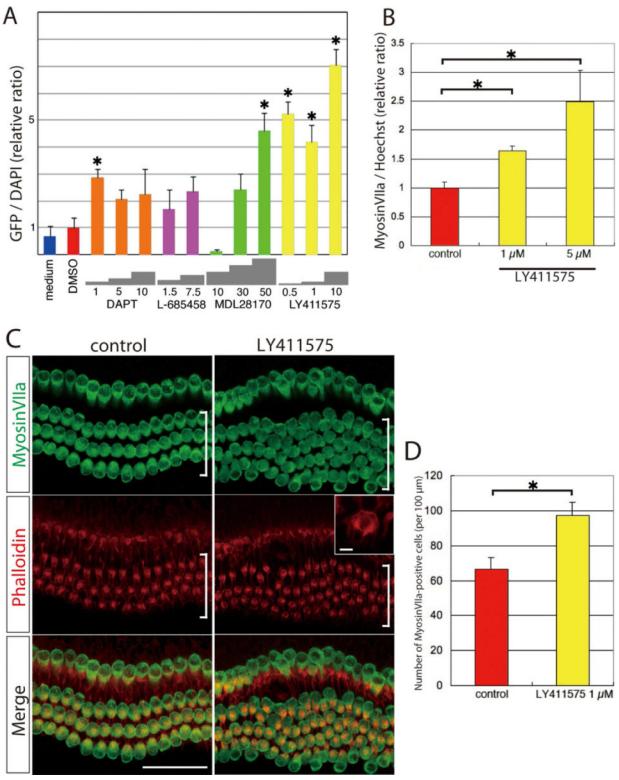

Figure 1. ***In vitro*** **activity of γ-secretase inhibitors in hair cell induction**

(A) Relative ratio of nGFP-positive cells to DAPI-positive cells after treatment of inner ear spheres made from *Math1-nGFP* mice with γ-secretase inhibitors at the indicated concentrations (μM) reveals that LY411575 had the greatest potency of 4 inhibitors tested for hair cell induction. Data were normalized to control values obtained by addition of DMSO. Asterisks indicate $p < 0.01$.

(B) Ratio of myosin VIIa (labels hair cells) to Hoechst-positive cells induced by LY411575 was calculated relative to DMSO-treated spheres from organ of Corti.

(C) Explant cultures of the organ of Corti from P1 mice cultured for 72 h in the presence of DMSO or LY411575 (1 μM) had ectopic hair cells (myosin VIIa; green) in the outer hair cell region (white bracket). Ectopic hair cells were positive for phalloidin (labels the hair bundle and cuticular plate; shown in red). Inset is a high-power view (scale bar is 2 μM) of a phalloidin-stained hair cell showing bundle structure.

(D) An increase in myosin VIIa-positive cells per 100 μm of the cultured organ of Corti explants from P1 mice was found 72 h after LY411575 treatment.

In all graphs, error bars show the standard error of the mean. Scale bar is 50 μm.

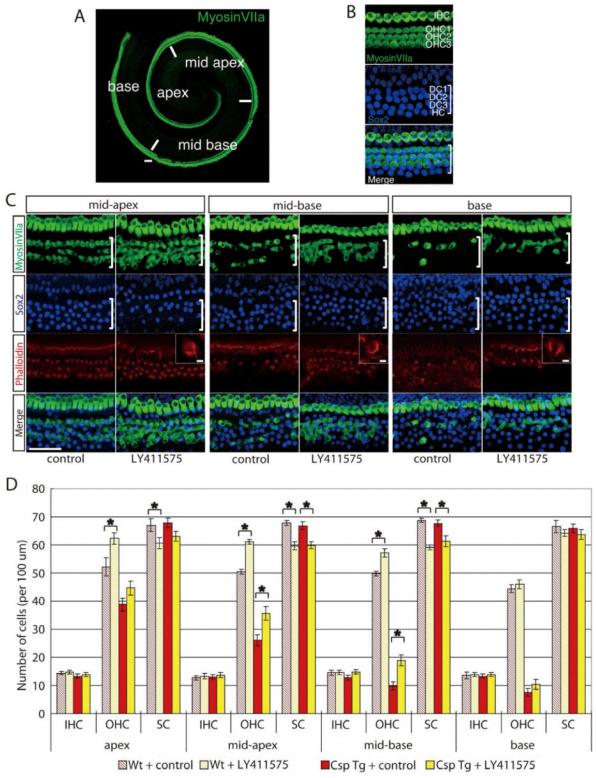

Figure 2. Hair cell replacement after LY411575 treatment of organ of Corti explants from mice subjected to ablation of hair cells

(A) Hair cells can be seen throughout the neonatal organ of Corti in a whole mount labeled for myosin VIIa.

(B) Three rows of outer (white bracket; OHC1 – 3) and one row of inner hair cells (IHC) can be seen in a P3 organ of Corti explant after staining for myosin VIIa. Deiters' cells (DC1 - 3) and Hensen cells (HC) in the outer hair cell region are positive for Sox2.

(C) Organ of Corti explants from *Pou4f3-Cre; Mos-iCsp3* double-transgenic mice subjected to dimerizer-induced hair cell ablation and cultured for 3 d in the presence of LY411575 had an increased number of myosin VIIa-positive cells in the outer hair cell region (white bracket) compared to the carrier-treated explant. The same region had a decreased number of Sox2-positive cells relative to the control. A high power view (scale bar, 2 μM) of phalloidin-stained tissue shows the hair cell stereociliary bundles (inset).

(D) The number of outer hair cells at the mid-apex and mid-base was increased in the LY411575 treated as compared to the control cochleae in the hair cell-ablated samples (Csp Tg). Increased numbers of hair cells were also seen after LY411575 treatment of wild-type organ of Corti (Wt) at the apex, mid-apex and mid-base. In both cases the increase in the number of hair cells was accompanied by a decrease in the number of supporting cells. The error bars are standard error of the mean (n = 7 in each group). Asterisks indicate $p < 0.05$. All scale bars are 50 μm.

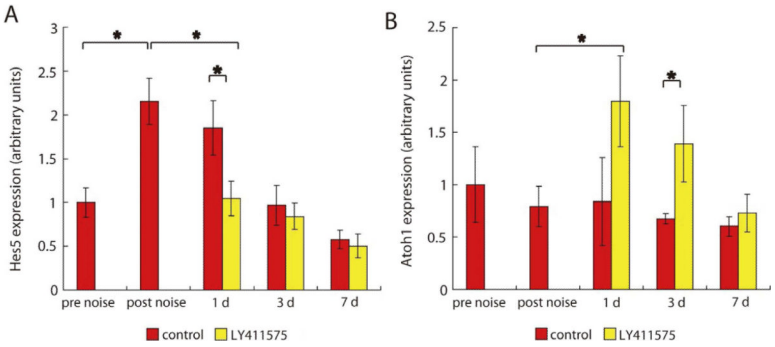

Figure 3. Time course of *Hes5* and *Atoh1* mRNA expression in the cochlea with or without LY411575 after noise exposure

(A) Elevated levels of *Hes5* after noise exposure were diminished in response to LY411575 treatment and reached the pre noise level. Without inhibitor, expression levels of *Hes5* in the cochlea increased 1 d after noise exposure and remained elevated compared to the pre noise level for up to 2 d. Samples for qRT-PCR were taken before exposure to noise (pre noise), at the time (day 0) of drug treatment (post noise), at day 1 of drug treatment (d 1), day 3 of drug treatment (d 3), and day 7 of drug treatment (d 7). mRNA expression levels were calculated relative to the pre-noise level.

(B) Treatment with LY411575 significantly increased the expression of *Atoh1* compared to the opposite, untreated ear 1 d after noise exposure. Increased levels were detected 1 d after drug treatment (d 1) and remained elevated 3 d after drug treatment (d 3; n = 9 in each group. Error bars are standard error of the mean. Asterisks indicate $p < 0.05$.

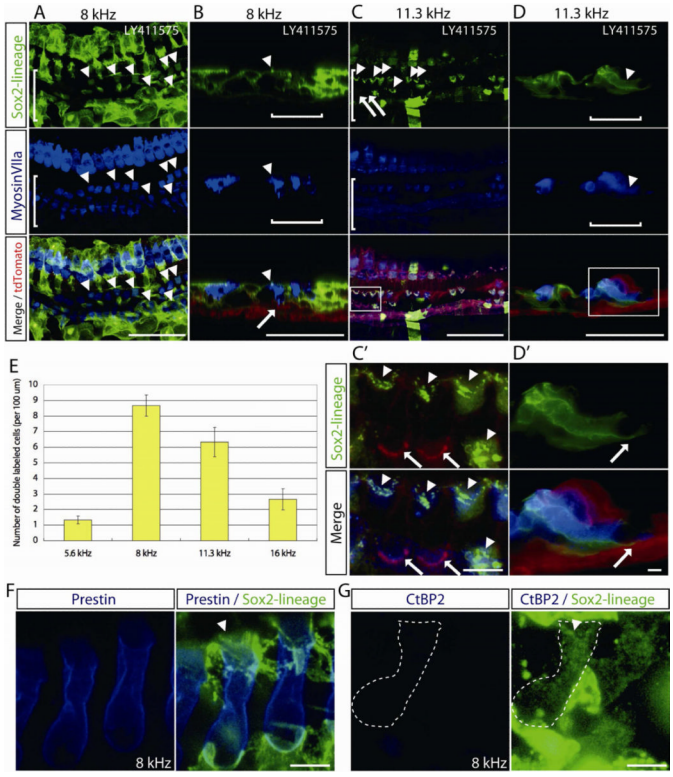

Figure 4. Lineage tracing of supporting cells in noise-exposed cochleae treated *in vivo* with a γ-secretase inhibitor

(A) Double-labeled cells (arrowheads) positive for Sox2 lineage (GFP) and myosin VIIa (blue) were observed in the outer hair cell area (white bracket) in cochlear tissues from deafened mice carrying the *Sox2-CreER* as well as the *Cre* reporter transgene, *mT/mG*, 1 month after LY411575 treatment. Hair cell co-labeling with the lineage tag indicates derivation from a Sox2-positive cell and is thus evidence for regenerated hair cells after deafening in the mature mouse cochlea by transdifferentiation of supporting cells. These confocal xy-projection images of LY411575-treated ears from *Sox2-CreER*; *mT/mG* double transgenic mice are in the 8 kHz area of the cochlear longitudinal frequency map.

(B) Confocal xz-projections from the same area as **A** show that myosin VIIa-positive cells in the medial part of the outer hair cell area (white bracket) had GFP-positive hair bundle structures, indicating a Sox2 lineage (arrowhead). The cell shown was attached to the basement membrane (arrow) similar to a supporting cell.

(C) Cells double-labeled for myosin VIIa (blue) and Sox2 lineage (green) were observed (arrowheads) in the outer hair cell area (white bracket) in the 11.3 kHz region in this xy projection from a deafened cochlea 1 month after LY411575 treatment. Original hair cells have red hair bundles and new, Sox2-lineage hair cells have green (GFP-positive) bundles.

(C') High power view of hair cells with their original (red) bundles (arrows) adjacent to cells with new (green) bundles (arrowheads) derived from Sox2-positive cells.

(D) Cross section from the same area as **C** shows that myosin VIIa, Sox2-lineage double-labeled cells in the outer hair cell area (white bracket) spanned the epithelium from the basement membrane to the endolymphatic surface.

(D') The cell shown is attached to the basement membrane (arrow) and its nucleus is at the base of the cell.

(E) Quantification of the GFP (Sox2 lineage) and myosin VIIa double-labeled cells in the outer hair cell region 1 month after treatment with LY411575 in deafened mice at

frequency-specific cochlear areas (n = 5 in each group). Error bars are standard error of mean.

(F) Cells double-labeled for prestin (blue) and Sox2 lineage (green) were observed in the 8 kHz region in this xy projection from a deafened cochlea 1 month after LY411575 treatment. Sox2-lineage hair cell has green (GFP-positive) bundles (white arrowhead).

(G) Sox2-lineage hair cells (white broken line) were negative for CtBP2, which labels inner hair cell synaptic ribbons. White arrowhead indicates hair cell bundle.

A–D: Scale bars are 50 μm. F, G: Scale bars are 5 μm.

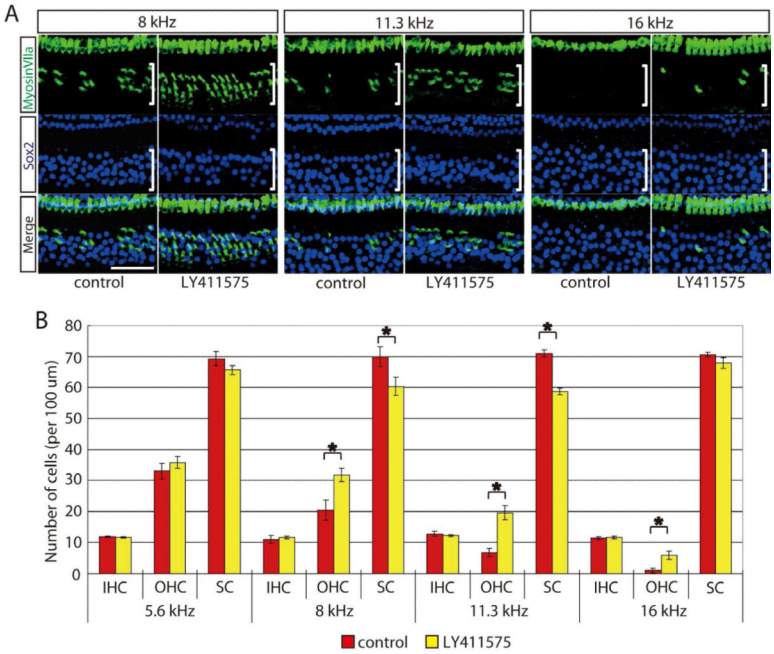

Figure 5. Hair cells in damaged mature cochlea treated with LY411575 *in vivo*

(A) The number of hair cells (green; myosin VIIa) in the outer hair cell region (white brackets) of deafened cochleae at 8, 11.3, and 16 kHz areas was increased compared to the control ear (right ear treated with carrier) 3 months after treatment with LY411575 (left ear), and the increase was accompanied by a decrease in the number of supporting cells (blue: Sox2) in the same regions in these whole mount confocal xy-projections.

(B) Significant differences in the numbers of hair cells and supporting cells were observed in the outer hair cell area at 8 and 11.3 kHz regions of treated (left) ears 3 months after treatment with LY411575 as compared to the values in the contralateral carrier-treated ear of deafened mice (n = 5 in each group).

All scale bars are 50 μm. Error bars are standard error of the mean and asterisks indicate $p < 0.05$.

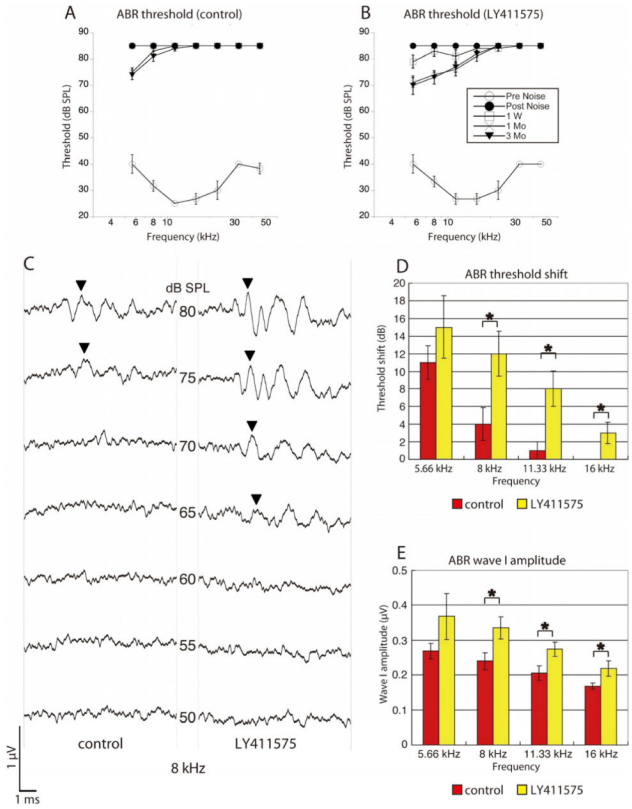

Figure 6. Measurement of ABR in deafened ears after LY411575 treatment

(A, B) A decrease in ABR thresholds at low frequencies (up to 16 kHz) in the left, LY411575-treated ear (B) compared to the right, control ear (A) was apparent in ABR thresholds in recordings made at 7 frequencies from 5.66 to 45.25 kHz with the following time course. Before noise exposure (Pre Noise: *open circles*), 1 d after noise exposure (Post Noise: *filled circles*), 1 week after drug treatment (1 W: *open squares*), 1 month after treatment (1 Mo: *crosses*), and 3 months after treatment (3 Mo: *filled triangles*) (n = 5 in each group). When no response was observed at 80 dB (maximum acoustic output of the system) the threshold was designated as 85 dB.

(C) An example of 8 kHz ABR waves recorded 3 months after drug treatment from the same mouse. Arrowheads show the peaks with the largest peak-to-peak amplitude. In the LY411575-treated ear, the peak could first be detected at 65 dB, while on the control side the peak could first be detected at 75 dB.

(D, E) The differences in threshold (D) and wave I amplitude (E) 3 months after drug treatment compared to 1 d after noise exposure between control and LY411575-treated ears at 8, 11.33, and 16 kHz (asterisks) were significant (n = 5 in each group).

Error bars are standard error of the mean.